A Mesh Deformation Algorithm for Free Surface Problems

by Gordon A. Fenton[1], and D. V. Griffiths[2]

Abstract

Employing the simple iterative technique of adjusting the element positions using computed potentials to locate the free surface can lead to finite elements with large aspect ratios as the free surface drops towards the base of the mesh. In particular, free surface modeling of earth dams with base drains suffer from this problem. The paper suggests a number of steps which can be taken to alleviate mesh distortion problems and improve the numerical stability of the iterative finite element analysis. This leads to a mesh deformation algorithm which adjusts element widths in a simple fashion depending on the free surface height as the iterations proceed. The algorithm is specialized to the sloped earth dam problem, but may find application to other geometries.

1. Introduction

In the finite element analysis of free surface flow, there are two main approaches; 1) fixed mesh algorithms (see e.g. Bathe and Khoshgoftaar, 1979, Rank and Werner, 1986, and Lacy and Prevost, 1987) in which the element properties are iteratively adjusted within a fixed mesh to reflect the location of the free surface, and 2) adaptive mesh algorithms (see e.g. Finn, 1967, Chung and Kikuchi, 1987, Cividini and Gioda, 1990, and Smith and Griffiths, 1988) in which the element properties are held constant while the mesh is iteratively deformed to match the free surface profile. In this approach, the determination of the free surface in an earth dam, as illustrated in Figure 1, proceeds by iteratively adjusting the element heights to equal their computed potential above a fixed datum (Smith and Griffiths, 1988). In that the adaptive mesh algorithm is very simple, requiring only the finite element implementation of Darcy's Law and an add-on mesh deformation procedure,

[1] Associate Professor, Technical University of Nova Scotia, Halifax, NS, B3J 2X4
[2] Professor, Colorado School of Mines, Golden, CO 80401

it was selected for use in a number of earth dam studies performed by the authors (Fenton and Griffiths, 1996). However, it soon became apparent, in the presence of sloped boundaries and/or drains at the base of the dam, that the elements could become severely distorted during the iterations, leading to numerical instabilities and slow convergence. This motivated a search for techniques of improving stability and reducing element distortion while still obtaining accurate results with reasonable efficiency and without resorting to more general adaptive mesh generators.

Figure 2 illustrates how the mesh can be distorted in the case where the original undeformed mesh (prior to the free surface iterations) is as shown in Figure 1. Since some of the elements achieve very large aspect ratios and interior angles close to 180^o, the analysis becomes numerically unstable leading to the convergence failure seen in the sequence of Figure 2. The free surface problem illustrated in Figure 2 arises from a random permeability field, the randomness serving to aggravate the problem by changing a relatively smoothly varying free surface into a rougher profile.

A number of possible approaches to reducing the numerical error suggest themselves;

1) increase the number of elements, particularly in the horizontal direction,
2) insist that the free surface be strictly non-increasing in the downstream direction.
3) adjust the spacing of the elements so that aspect ratios do not become so large as the free surface drops,
4) smooth, damp, or average the results of previous iterations to avoid wild swings in the predicted response,

The first approach, while valid, may entail a very large number of elements in cases where the free surface descends significantly. It is an approach more suited to the case where the approximate free surface location is known *a-priori*, but otherwise results in a significant computational penalty (which, in a stochastic framework, is to be avoided). Although this is the simplest solution, this paper addresses the other approaches primarily to avoid the inefficiency associated with a large number of elements.

The second suggestion, insisting that the free surface be strictly non-increasing and adjusting its location if not, may be a reasonable stipulation in the case where the permeability through the dam is everywhere constant. However, it suffers from a number of disadvantages; first, by arbitrarily adjusting the free surface location so that it is strictly non-increasing may result in convergence to an incorrect location if numerical errors are persistent. Second, the free surface may show local increases in the case where the permeability field is spatially random, so that the stipulation is not correct in this case. However, this is a quick and simple fix that usually results in a fast convergence to a reasonable approximation, and, for example, eliminates the non-convergence observed in Figure 2.

The third approach is reported in greater detail in the following sections of the paper. If the spacing adjustment is properly implemented, the fourth suggestion, which serves primarily to accelerate convergence in pathological cases, is not usually necessary but suggestions as to its implementation, based on empirical observations, will be made.

2. Free Surface Iterations

The advantage of the iterative mesh deformation algorithm, where the elevation of the upper surface of the mesh is equated to the potential (both measured from some fixed elevation) computed in the previous iteration, is that it clearly converges to the correct result when the implementation of Darcy's Law is accurate. This is both in the sense of iterations using a fixed mesh and in the usual sense of the finite element discretization where the error reduces as the mesh is refined to some lower round-off error floor. The quadrilateral Darcy element is accurate so long as it does not become too severely distorted, thus the overall algorithm's success is ensured if the elements shapes are adjusted to avoid severe distortion or large aspect ratio.

The first task is to properly adjust nodal positions, given a computed potential field from the previous iteration. When the domain is rectangular and nodes lie along vertical lines, this is simply a matter of adjusting the vertical position of the nodes. It is, however, somewhat more complicated

when the flow domain is bounded by sloped lines. In the following, it will be assumed that nodes lie along non-intersecting straight lines connecting the top and bottom surfaces of the domain. This geometry implies that the dam must be a truncated pyramid unless triangular elements are employed. Since, in the case of earth dams, one need only model at and below the free surface, the truncation is not usually a restriction and quadrilateral elements can be used.

Consider the geometry shown in Figure 3, where the domain is discretized into n_{xe} elements horizontally by n_{ye} elements vertically. The variables b_i and t_i give the x-coordinates of the base and top nodes, respectively, for $i = 1, 2, \ldots, n_{xe} + 1$. The overall domain height is y_h, base width is x_{bot}, and top width is x_{top}. For simplicity, it will be assumed that the top is centered over the base. Each nodal pair having coordinates $(b_i, 0)$ and (t_i, y_h) is connected by a straight line. Along this line, $n_{ye} + 1$ nodes are distributed with elevations to be determined as follows. If s_i is the potential computed in the current finite element iteration at the i'th node along the top surface, and hence the target elevation of the i'th node in the next iteration, then the x-coordinate of the i'th node is given by

$$c_i = b_i + \left(\frac{s_i}{y_h}\right)(t_i - b_i)$$

so that the free surface nodal position, obtained by sliding along the line connecting $(b_i, 0)$ and (t_i, y_h), has coordinates (c_i, s_i).

If the computed potential s_i is sufficiently small, then the elements may achieve very large aspect ratios since they are compressed into a small elevation. Ideally, the width of the element should be adjusted to become approximately the same as its height. In general, this can only be done properly by changing the number of elements in the mesh. Changing the number of elements 'on the fly' involves a much more complicated bookkeeping algorithm, mapping degrees-of-freedom to boundary conditions, etc., which would have to be implemented and re-invoked on each iteration. To avoid this additional complexity and overhead it was decided to maintain a fixed number of elements and adjust their spacing more simply – gradually increasing in the upstream direction.

A number of spacing algorithms were considered;

1) element width proportional to the free surface elevation above the element (at the top of the column of elements, which may be sloped). The proportionality constant is determined by requiring that the sum of element widths equal the dam width;

$$r = \frac{x_{bot}}{\sum_{i=1}^{n_{xe}}(s_i + s_{i+1})}$$
$$b_i = b_{i-1} + r(s_{i-1} + s_i) \qquad i = 2, 3, \ldots, n_{xe}$$

The top nodes are shifted analogously, using x_{top} and t_i instead of x_{bot} and b_i.

2) linearly increasing element widths with narrowest element at downstream face having width determined by the downstream free surface elevation, as follows;

$$r = \left(\frac{s_1}{y_h}\right)^2$$
$$d = \frac{x_{bot}}{n_{xe}}$$
$$e = \frac{2d(1-r)}{n_{xe}-1}$$
$$b_i = b_1 + (i-1)\left(rd + \tfrac{1}{2}(i-2)e\right), \qquad i = 2, 3, \ldots, n_{xe}$$

Smaller values of r decrease the width of the downstream element. For a fixed free surface elevation ratio, s_1/y_h, empirical testing showed that the reduction in r needed to be amplified to get reasonable results which is why the ratio is squared above. The top nodes are shifted analogously, using x_{top} and t_i instead of x_{bot} and b_i.

3) geometrically increasing element widths with narrowest element at downstream face having width determined by the amount of drawdown, s_1/y_h. This model shifts the base nodes as follows;

a) compute $d_{bot} = \frac{s_1}{n_{ye}}$ as the width of the downstream base element,

b) if $d_{bot} < \frac{x_{bot}}{n_{xe}}$ then

- compute $d_{top} = d_{bot}\left(\frac{x_{top}}{x_{bot}}\right)$
- find root of $f(\alpha) = \frac{\alpha-1}{\alpha^{n_{xe}}-1} - \frac{d_{bot}}{x_{bot}} = 0$

- $b_i = b_1 + \left(\frac{\alpha^{i-1}-1}{\alpha-1}\right) d_{bot}, \qquad i = 2, 3, \ldots, n_{xe}$
- $t_i = t_1 + \left(\frac{\alpha^{i-1}-1}{\alpha-1}\right) d_{top}, \qquad i = 2, 3, \ldots, n_{xe}$

Since $1 < \alpha < (x_{bot}/d_{bot})^{\frac{1}{n_{xe}-1}}$, the root is conveniently found using bisection (for this function, bisection is also more efficient than, say, Newton-Raphson).

Once the base and top nodes have been shifted according to the above discussion, the final free surface and, in fact, all the remaining nodes, must be transferred to the new set of lines joining $(b_i, 0)$ and (t_i, y_h). To define the new free surface, that is to find the location of each node i along the free surface, the index $1 \leq j \leq n_{xe}$ is found so that the line segments between the points $[(b_i, 0), (t_i, y_h)]$ and $[(c_j, s_j), (c_{j+1}, s_{j+1})]$ cross each other. This intersection becomes the locus of the new free surface. All other nodes are distributed evenly below the new free surface. The algorithm to find the free surface is as follows;

a) set j = 1

b) for $i = 2, 3, \ldots, n_{xe}$ do

1) $d = (s_j - s_{j+1})(t_i - b_i) + y_h(c_{j+1} - c_j)$

2) if d = 0 then ERROR: the lines do not intersect – convergence failure

3) $\xi = \Big(s_j(t_i - b_i) + y_h(b_i - c_j)\Big)/d$

4) if $\xi < 0$ or $\xi > 1$ then check next free surface line segment;

i) set $j = j + 1$

ii) if $j > n_{xe}$ then ERROR: unable to find free surface

iii) return to step (1)

else

i) $x_i = [(c_{j+1}s_j - c_j s_{j+1})(t_i - b_i) + b_i y_h(c_{j+1} - c_j)]/d$

ii) $y_i = y_h[b_i(s_{j+1} - s_j) + (c_{j+1}s_j - c_j s_{j+1})]/d$

endif

enddo

where (x_i, y_i) are the updated coordinates of the free surface. The bound $\xi > 1$ may be changed to $\xi > (1 + \epsilon)$, for suitably small ϵ, to avoid not finding an intersection due to round-off error. The two error conditions noted above should never occur.

In the case of geometric or linear element spacing, one final check is applied by looking at the overall aspect ratio of the uppermost downstream element. If this aspect ratio exceeds 5, then the effective downstream free surface elevation is taken to be $s_1/2$ and the spacing algorithm repeated. This strategy was found to be necessary only occasionally but did further reduce the number of divergent cases to be discussed later.

With a random permeability field, convergence is sometimes slow to occur due to the mapping of permeabilities from the spatially fixed permeability field to the deforming finite element mesh. If the permeability mapped to a given element flops back and forth as it shifts slightly (spatially), then the free surface may continue to oscillate from iteration to iteration. To alleviate this situation, the response computed on each iteration is damped to give an 'averaged' computed free surface of

$$i_d = \max(k - 16, 1)$$

$$\beta = \sqrt{1/i_d}$$

$$s_i = (1 - \beta)s_i + \beta\phi_i$$

in which k is the iteration count and ϕ_i is the potential computed at the i'th node along the free surface. In this formulation, the first 16 iterations are left undamped. The number 16 was selected after some trial and error, considering overall average convergence rates. The use of a square root in the calculation of β reduces the rate of increase of the damping. It was found that using, for example, $\beta = 1/i_d$ often resulted in non-convergence simply because the effect of successive iterations became too rapidly negligible. For most permeability realizations, convergence is attained before damping is necessary.

The various element spacing methods were tested on a suite of 100 realizations of a random permeability field applied to the earth dam geometry shown in all the figures. Divergence, due to

excessive element distortion, is identified whenever the computed free surface exceeds 1.2 times the dam height or dips below the dam baseline. Diverged flow profiles typically resemble that shown in Figure 2 and yield unusable results.

The maximum number of iterations was set at 80, after which the analysis was discontinued and considered to be an unconverged case. Convergence was attained when the max-norm relative error on the entire free surface elevation became less than 0.5%. In general, unconverged flow profiles were not found to differ much from those obtained by allowing more iterations (with damping) so that non-convergence is usually not a major concern.

Two cases were considered; 1) an earth dam with a drain running along the dam base from the centerline to the downstream face, and 2) an earth dam without a drain. The free surface tends to exit somewhere about half height of the dam in the second case and typically results in elements near the top downstream corner with interior angles approaching 180^{o} since the free surface often approaches the downstream face at a tangent. In the presence of a drain, the free surface descends rapidly, getting quite close to the base and potentially yielding very large element aspect ratios. Table 1 tabulates the number of unconverged, divergent, and the average number of iterations (convergent cases) over the 100 realizations. Figure 4 illustrates the converged results obtained using the geometric spacing algorithm for the drained and undrained earth dam. The undrained case of Figure 4(a) corresponds to the same permeability field which led to the failure in Figure 2.

3. Conclusions

Of the various mesh shifting techniques considered in this study, the one which showed overall the least divergence and best convergence rates was that of geometric shifting. Although not reported here, the method has been used for a variety of dam side slopes, with and without base drains, for a variety of discretizations, and under various random permeability field statistics. The average convergence rate was about the same for all spacing methods, including the no spacing adjustment case. The latter had by far the largest number of divergent results, motivating this study. For

earth dams without drains, where the free surface remains relatively high, the linear or proportional spacing algorithms showed the best results with geometric spacing having about 1% divergent cases. In the presence of a drain, geometric spacing was superior. The proportional spacing gave good results without a drain, but was significantly slower with a high number of unconverged results in the presence of a drain.

The algorithms given in this paper can be used by those wishing to use quadrilateral elements in an iterative free surface problem without having to resort to adaptive mesh generators. Since the permeability fields which resulted in failure of the geometric spacing algorithm often differed from those causing failure of the linear spacing algorithm, one possible application of these methods is to use geometric spacing and switch over to linear spacing in the event of divergence. Finally, convergence can be assured in all cases by restricting the free surface to be non-increasing in the downstream direction. This, however, may result in convergence to an incorrect result unless it is known *a-priori* that the free-surface is non-increasing.

4. Acknowledgements

Thanks for financial support are due to the Natural Sciences and Engineering Research Council of Canada under Grant OPG0105445 as well as to the United States National Science Foundation under Grant 4-41589. Any opinions, findings, and conclusions and recommendations are those of the authors and do not necessarily reflect the views of the aforementioned organizations.

REFERENCES

Bathe, K.J. and Khoshgoftaar, M.R. (1979). "Finite element free surface seepage analysis without mesh iteration," *Internat. J. Numer. Anal. Methods Geomech.*, **3**, 13–22.

Chung, K.Y. and Kikuchi, N. (1987). "Adaptive methods to solve free boundary problems of flow through porous media," *Internat. J. Numer. Anal. Methods Geomech.*, **11**(1), 17–32.

Cividini, A. and Gioda, G. (1990). "On the variable mesh finite element analysis of unconfined seepage problems," *Géotechnique*, **40**(3), 523–524.

Fenton, G.A. and Griffiths, D.V. (1996). "Statistics of free surface flow through stochastic earth dam," *ASCE J. Geotech. Eng.*, **122**(6), 427–436.

Finn, W.D.L. (1967). "Finite element analysis of seepage through dams," *ASCE J. Soil Mech. Found. Div.*, **93**(SM6), 41–48.

Lacy, S.J. and Prevost, J.H. (1987). "Flow through porous media: A procedure for locating the free surface," *Internat. J. Numer. Anal. Methods Geomech.*, **11**(6), 585–601.

Rank, E. and Werner, H. (1986). "An adaptive finite element approach for the free surface seepage problem," *Internat. J. Numer. Methods Engrg.*, **23**(7), 1217–1228.

Smith, I.M. and Griffiths, D.V. (1988). *Programming the Finite Element Method*, John Wiley & Sons, New York, NY.

NOTATION

The following symbols are used in this paper:

b_i = x-coordinate of the i'th node along the dam base

c_i = x-coordinate of the i'th node along the free surface

n_{xe} = number of elements in the x (horizontal) direction

n_{ye} = number of elements in the y (vertical) direction

s_i = vertical elevation of the i'th node along the free surface

t_i = x-coordinate of the i'th node along the dam top

x = horizontal coordinate axis

x_{bot} = width of the dam base

x_{top} = width of the dam top

y = vertical coordinate axis

y_h = vertical height of the dam, also upstream free surface elevation

Table 1. Convergence results over 100 random permeability field realizations for various spacing algorithms.

Method	**Without Drain**			**With Drain**		
	Unconverged (%)	Diverged (%)	Ave. Number of Iterations	Unconverged (%)	Diverged (%)	Ave. Number of Iterations
None	0	8	12	0	16	15
Geometric	0	1	12	0	0	15
Linear	0	0	13	0	4	15
Proportional	0	0	12	13	0	29

Figure 1. Finite element mesh of earth dam (a) with example realization of permeability field and free surface (b).

Figure 2. Divergent iteration sequence (a through d) due to excessive element distortion.

Figure 3. Earth dam dimensions illustrating top and bottom nodal x-coordinate labeling.

Figure 4. Converged free surface results obtained using geometric spacing for undrained, (a), and drained, (b), earth dams.

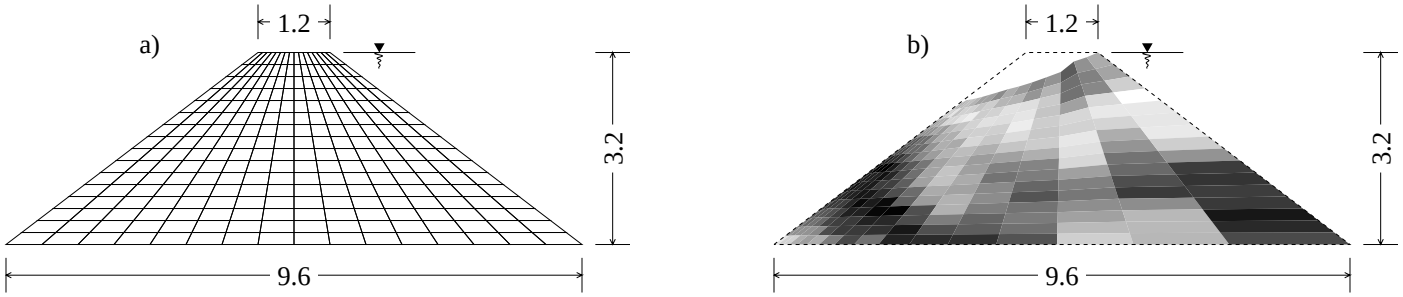

Figure 1 (Fenton/Griffiths)

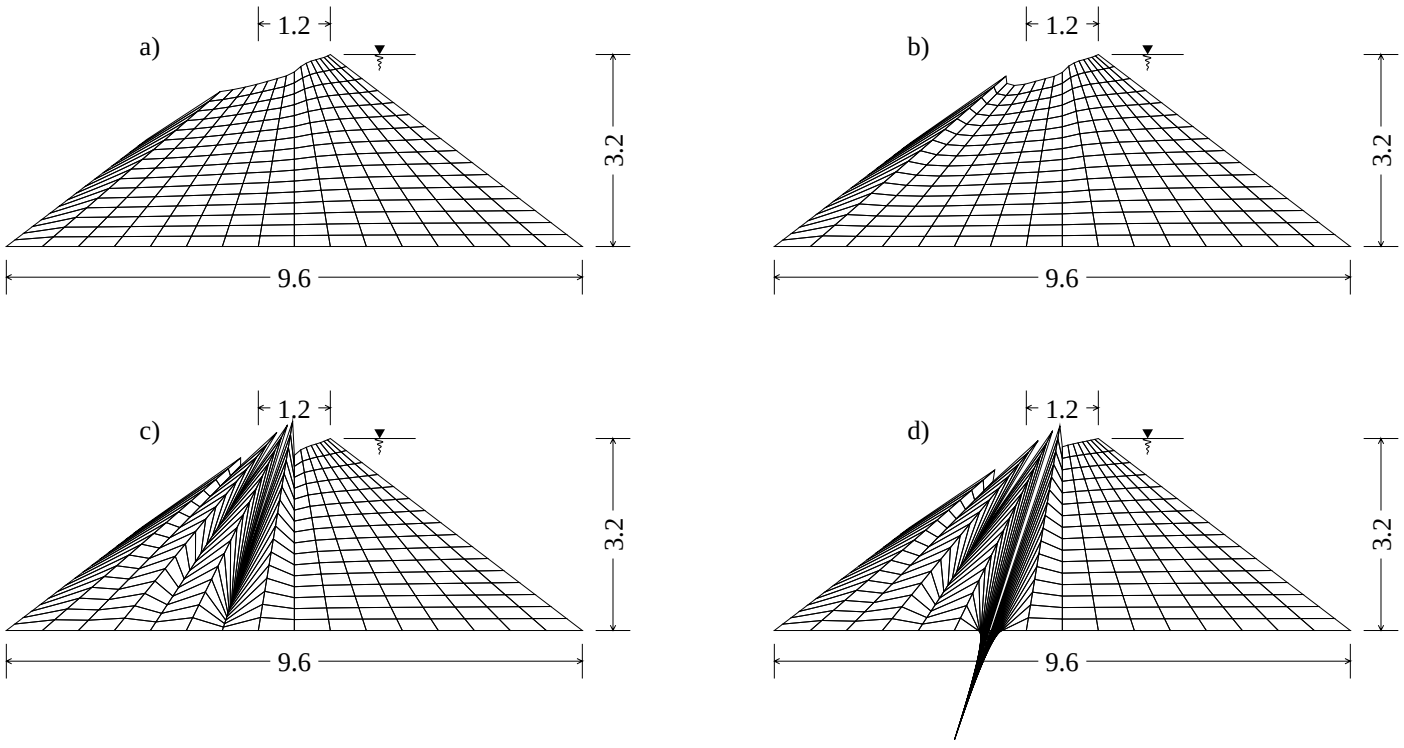

Figure 2 (Fenton/Griffiths)

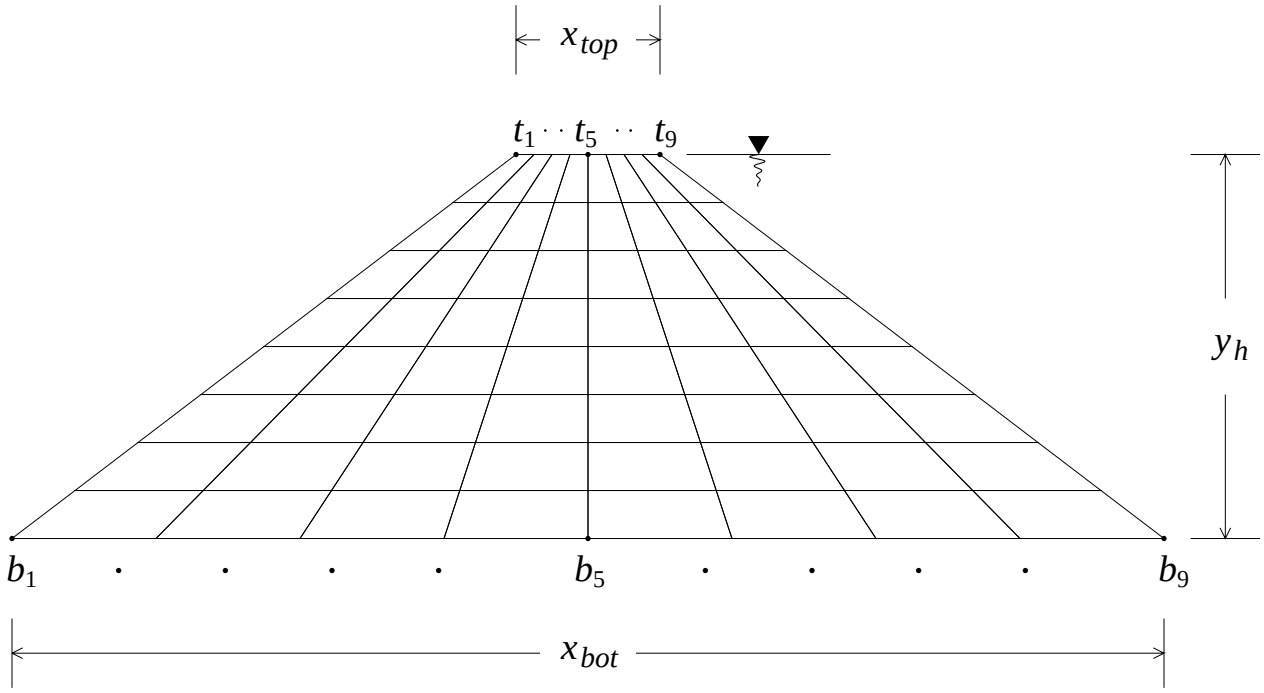

Figure 3 (Fenton/Griffiths)

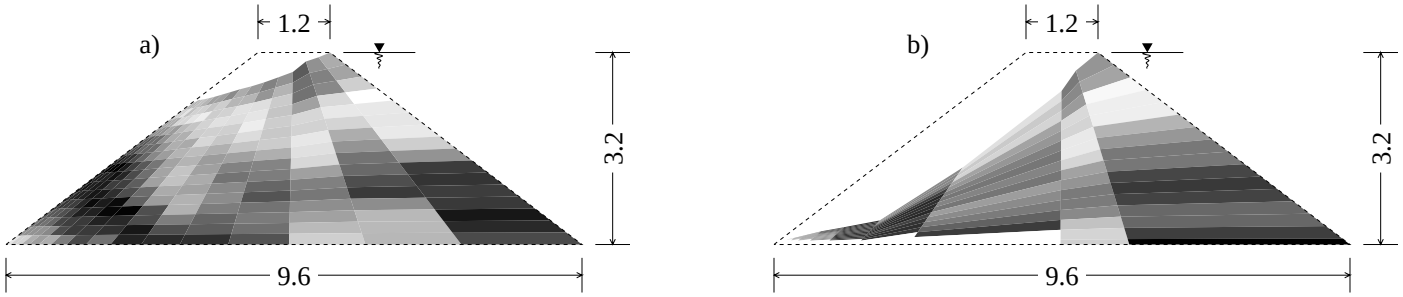

Figure 4 (Fenton/Griffiths)